Total and Methylated Mercury in Arctic Multiyear Sea Ice

ARTICLE *in* ENVIRONMENTAL SCIENCE & TECHNOLOGY · APRIL 2014

Impact Factor: 5.33 · DOI: 10.1021/es5008033 · Source: PubMed

6 AUTHORS, INCLUDING:

Sarah A. Beattie
University of Manitoba
4 PUBLICATIONS **23** CITATIONS
SEE PROFILE

Debbie Armstrong
University of Manitoba
11 PUBLICATIONS **165** CITATIONS
SEE PROFILE

Michel Gosselin
Université du Québec à Rimouski UQAR
184 PUBLICATIONS **5,355** CITATIONS
SEE PROFILE

Feiyue Wang
University of Manitoba
110 PUBLICATIONS **3,326** CITATIONS
SEE PROFILE

Environmental Science & Technology

Article

pubs.acs.org/est

Total and Methylated Mercury in Arctic Multiyear Sea Ice

Sarah A. Beattie,[†] Debbie Armstrong,[†] Amanda Chaulk,[†] Jérôme Comte,[‡] Michel Gosselin,[§] and Feiyue Wang*[,†]

[†]Center for Earth Observation Science, Department of Environment and Geography, University of Manitoba, Winnipeg, MB R3T 2N2, Canada

[‡]Takuvik Joint International Laboratory, Centre national de la recherche scientifique (France, CNRS UMI 3376), Centre d'études nordiques, Département de biologie, and Institut de biologie intégrative et des systèmes, Université Laval, Québec, QC G1V 0A6, Canada

[§]Institut des sciences de la mer de Rimouski, Université du Québec à Rimouski, Rimouski, QC G5L 3A1, Canada

Supporting Information

ABSTRACT: Mercury is one of the primary contaminants of concern in the Arctic marine ecosystem. While considerable efforts have been directed toward understanding mercury cycling in the Arctic, little is known about mercury dynamics within Arctic multiyear sea ice, which is being rapidly replaced with first-year ice. Here we report the first study on the distribution and potential methylation of mercury in Arctic multiyear sea ice. Based on three multiyear ice cores taken from the eastern Beaufort Sea and McClure Strait, total mercury concentrations ranged from 0.65 to 60.8 pM in bulk ice, with the highest values occurring in the topmost layer (~40 cm) which is attributed to the dynamics of particulate matter. Methylated mercury concentrations ranged from below the method detection limit (<0.1 pM) to as high as 2.64 pM. The ratio of methylated to total mercury peaked, up to ~40%, in the mid to bottom sections of the ice, suggesting the potential occurrence of in situ mercury methylation. The annual fluxes of total and methylated mercury into the Arctic Ocean via melt of multiyear ice are estimated to be 420 and 42 kg yr^{-1}, respectively, representing an important and changing source of mercury and methylmercury into the Arctic Ocean marine ecosystem.

INTRODUCTION

High concentrations of mercury (Hg) have been reported within tissues of Arctic marine mammals,[1] raising health concerns for the animals as well as the Northern People who rely on the animal tissues as part of their traditional diet.[2] The extensive research efforts that have ensued found high spatial and temporal variability of Hg in upper trophic-level marine biota, which cannot be fully explained by atmospheric loading histories alone.[3,4] It has been suggested that changes within the Arctic system have altered postdepositional biogeochemical processes that dictate the transport, transformation, and biological uptake of Hg in the Arctic Ocean.[4−6] Processes that require immediate attention are those which produce or release monomethylmercury (including CH_3Hg^+ and its complexes, hereafter MMHg), the primary Hg species that causes biological concerns due to its neurotoxicity and biomagnifying nature.[7] Arguably the most dramatic change the Arctic Ocean has undergone recently is the shift in composition of the icescape. Record low summer sea ice extent events, as observed in 2007 and 2012, demonstrate the extensive loss of multiyear (MY) ice and continue to compromise the resilience of the permanent icepack.[8−11] This signifies a shift from a MY to a first-year (FY) ice regime, yet the effects of this shift on the biogeochemical cycling of Hg in the Arctic Ocean system remain unknown.

Arctic sea ice is a heterogeneous, multiphase matrix composed of ice, brine, gases, minerals, particulate matter, and biota (e.g., bacteria, viruses, algae).[12,13] After initial nucleation and formation, ice growth and evolution is driven by various physical, chemical, and biological processes which govern the micro- and macroproperties of sea ice.[12,13] Brine pockets and drainage channels increase the permeability of sea ice to the transport of gases, solutes, and particulate matter, with vertical fluid permeability being a function of porosity and brine volume fraction, which are in turn a function of temperature and salinity of the bulk ice.[12,13] Recent studies on FY ice have found Hg to heavily concentrate in the brine phase, and therefore the fluid dynamics of the brine strongly influences Hg distribution and transport within the ice column.[14,15] This characteristic has strong implications when considering the brine dynamics of FY and MY ice. The evolution of MY ice through the melt season is driven by two

Received: February 16, 2014
Revised: April 21, 2014
Accepted: April 27, 2014
Published: April 28, 2014

   dx.doi.org/10.1021/es5008033 | Environ. Sci. Technol. 2014, 48, 5575−5582

distinct processes: desalination and crystal retexturing.[16] The enhanced brine dynamics of MY ice will likely influence Hg distribution within the ice column and transport across the ocean−sea ice−atmosphere interface. Although the distribution of Hg in young and FY ice has been studied in some detail,[14,15] so far the Hg distribution profile in MY ice has only been reported for a single core collected in 2008.[14]

Of particular pertinence is the recent discovery of local anaerobic conditions within sea ice.[17,18] It is well established that the production of MMHg is favored in redox transition zones where some dissimilatory sulfate-reducing bacteria and iron-reducing bacteria thrive.[19] However, high MMHg concentrations have also been reported in Arctic seawater[7,20,21] and snow[21−23] where anaerobic conditions are uncommon.[19] Sea ice has been shown to support higher bacterial activity than underlying seawater.[24] Despite a recent measurement of MMHg in Antarctic FY ice,[15] it remains unknown whether Hg methylation occurs in situ in sea ice.

This paper aims to better define the role of MY ice in the biogeochemical cycling of Hg in the Arctic Ocean by investigating its potential as a transformation medium for MMHg production, and as a source of Hg and MMHg into the marine ecosystem. The processes governing Hg distribution within MY ice is also assessed. To our knowledge this work represents the first measurement of MMHg in MY ice.

MATERIALS AND PROCEDURES

Sampling and Sample Preparation. The sea ice cores were retrieved from MY ice floes in the eastern Beaufort Sea and McClure Strait of the Arctic Ocean (Figure 1, Table 1), where the median September old ice (essentially all MY ice) concentration, expressed as aerial coverage, ranged from 7−10/10 and 4−6/10, respectively, for the period 1981−2010 (Canadian Ice Service; http://ec.gc.ca/glaces-ice). Details of the study area can be found in the Supporting Information (SI).

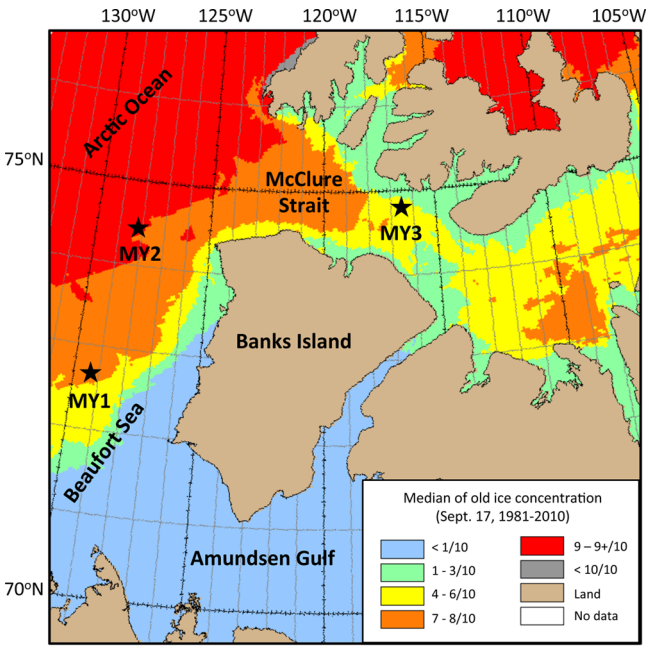

Figure 1. Locations of multiyear sea ice sampling sites MY2 (August 16, 2011) and MY3 (September 9, 2013), overlaid onto a 30-yr sea ice climatic atlas of median old ice concentration for September 17 (1981−2010) generated by Canadian Ice Service of Environment Canada (http://ec.gc.ca/glaces-ice). Also shown is the location of MY1 from an earlier study (May 25, 2008[14]).

The first MY ice site, MY1 (ice thickness: 350 cm; snow depth: 23 cm), was cored on May 25, 2008 in the eastern Beaufort Sea, for which total Hg data have been reported in an earlier study;[14] it was not analyzed for MMHg. Two new MY sites were cored in this study. MY2 (ice thickness: 370 cm; snow had all been melted) was carried out on August 16, 2011 in the northeastern Beaufort Sea, and MY3 (ice thickness: 270 cm; snow depth: 5 cm) on September 9, 2013 in McClure Strait. All the coring was carried out during ArcticNet cruises of the Canadian Research Icebreaker CCGS Amundsen. At the time of sampling, the MY floe at MY2 showed deformed surfaces and melt ponds; in contrast, melt ponds were not visible within the immediate vicinity of MY1 and MY3, though the ice surfaces possessed rolling features.

All cores were collected using a Mark II Kovacs core barrel (i.d. = 9 cm, with aluminum cutting shoe and stainless steel cutting teeth) in 1 m sections. At each site, four replicate ice cores spanning the entire ice thickness were taken from areas where the overlying snowpack had been removed to bare ice surface. One replicate core was for the measurement of total Hg (Hg_T), one for total methylated Hg ($MeHg_T$), one for in situ temperature, and the fourth for salinity and other ancillary parameters. An additional core was taken at MY3 for bacterial enumeration. Sea ice temperature (T) was measured in situ immediately after core retrieval. Holes (~5 cm deep) were drilled at 10 cm intervals down the length of the core, and a Model 400 thermometer (precision: ±0.05 °C; Traceable Control Company) was inserted into each hole for measurement. To minimize the loss of brine, all other cores were placed into plastic bags immediately upon being removed from the floe and rapidly transported to the cold lab (−20 °C) onboard the icebreaker.

Once inside the cold lab, the ice cores were cut into 5 to 10 cm sections within 36 h of sampling. The cores for Hg_T and $MeHg_T$ analysis were halved to produce pseudoreplicates. The outer 1 cm layer of the cores was scraped off using precleaned ceramic blade knives (Kyocera) as described elsewhere.[14] Sampling and sample preparation strictly followed the clean-hands−dirty hands protocol[25] at the Portable In-situ Laboratory for Mercury Speciation (PILMS), a Class 100 cleanroom laboratory onboard the icebreaker. All sampling tools were precleaned and tested for acceptable background Hg levels (<0.5 pM) prior to use and doubly bagged separately in new Ziploc bags. Ultrapure Milli-Q Element water (Millipore) produced in PILMS was used as laboratory water. After being melted in PILMS, samples for Hg_T analysis were transferred into new 50 mL polypropylene Falcon tubes (BD) which had been shown to contain extremely low levels of background Hg;[14] nevertheless, random tests were carried out for every batch of new tubes. Samples were spiked with 250 μL of concentrated ultrapure HCl (JT Baker) and 250 μL of BrCl (prepared from KBr and $KBrO_3$, JT Baker, in ultrapure HCl) prior to analysis at PILMS onboard the ship. Samples for $MeHg_T$ analysis were transferred into 150 mL precleaned and pretested Teflon sample containers, packed into a large cooler (−10 °C) and shipped to the University of Manitoba for analysis.

The ice samples from the other replicate cores were melted under low-light conditions for the analysis of salinity, $\delta^{18}O$, dissolved organic carbon (DOC), chlorophyll *a* (Chl *a*), and bacterial enumeration. Subsamples for $\delta^{18}O$ analysis were

dx.doi.org/10.1021/es5008033 | Environ. Sci. Technol. 2014, 48, 5575−5582

Table 1. Total Mercury (Hg_T) and Total Methylated Mercury ($MeHg_T$) Concentrations in Arctic Multiyear Sea Ice (N/A: data not available)

						Hg_T (pM)			$MeHg_T$ (pM)		
site ID	location	date sampled (UTC)	surface conditions	snow depth (cm)	ice thickness (cm)	range	median	volume-weighted mean	range	median	volume-weighted mean
MY1	72.65°N, 129.44°W	25-May-2008	deformed surface; no melt ponds	23	350	1.10−21.8	2.79	4.04	N/A	N/A	N/A
MY2	74.50°N, 128.16°W	16-Aug-2011	highly deformed surface; melt ponds	0 (melted into ice)	370	0.65−49.2	3.64	5.58	<0.1−0.55	0.15	0.20
MY3	74.75°N, 116.42°W	09-Sept-2013	deformed surface; no melt ponds	∼5	270	3.39−60.8	10.9	12.7	0.75−2.64	1.30	1.35

decanted into 20 mL clear glass scintillation vials and stored at 4 °C in the dark until analysis. The subsample for DOC was filtered through precombusted (450 °C for 5 h) Whatman GF/F filters (0.7 μm nominal pore size). The filtrate was collected in 9 mL glass storage vials with Teflon-lined caps previously cleaned following the protocol of Burdige and Homstead[26] and acidified to ∼pH 2 with 100 μL of 2 M HCl. The DOC samples were kept at 4 °C in the dark until analysis. Subsamples for Chl *a* were also filtered through Whatman GF/F filters. Bacterial samples were fixed with 0.1% final concentration of glutaraldehyde, flash-frozen in liquid nitrogen for 1 h, and stored at −80 °C until analysis.

Analyses. Detailed analytical methods and quality control information are provided in SI. Briefly, Hg_T analysis was carried out in PILMS, within 24−36 h of core processing, by cold vapor atomic fluorescence spectroscopy (CVAFS) on a Tekran 2600 Hg analyzer in accordance with U.S. EPA Method 1631.[27] The method detection limit (MDL) was 0.05 pM, and Hg_T levels in field blanks were below <0.35 pM. Note that the Hg_T data reported is unfiltered and represent all Hg species (dissolved and particulate; inorganic and organic). $MeHg_T$ analysis was performed at the Class 100, metal-free Ultraclean Trace Elements Laboratory (UCTEL) at the University of Manitoba. Samples were stored in a dedicated chest freezer (−18 °C) and analyzed within 8 months of sampling. Analysis of $MeHg_T$ in MY2 samples followed U.S. EPA Method 1630.[28] Analysis of $MeHg_T$ in MY3 samples followed a similar procedure except without the distillation process as described in Bowman and Hammerschmidt.[29] The MDL for both methods was 0.1 pM, and field blanks were <0.2 pM. Note that under acidic preservation conditions, dimethylmercury (DMHg) will rapidly decompose to MMHg, and thus $MeHg_T$ data reported here represent the sum of MMHg and DMHg[7] in unfiltered, melted bulk sea ice.

Bacterial enumeration and analyses of single-cell characteristics were carried out using a FACScalibur flow cytometer (Becton Dickinson), equipped with an argon laser. Samples were processed at the lowest flow rate (12 μL min^{-1}), using 1 μm yellow green microspheres (Polysciences) solution as the internal standard. Beads concentration was controlled using Truecount Absolute counting tubes (BD Biosciences). For total counts and the enumeration of cells with high (HNA) or low (LNA) nucleic acid content, samples were stained with a 40 μL mL^{-1} of nucleic acid dye SYBR Green I for 10 min in the dark. Stained cells were then discriminated on the basis of their green fluorescence at 530 nm (FL1) and their 90 °C light scatter signals while being excited at 488 nm. Manual gating was used to discriminate both HNA and LNA fractions. Data were analyzed using the CellQuest Pro software.

Analysis of $\delta^{18}O$, DOC, and Chl *a* followed well-established methods which are described in SI. Salinity of the bulk ice was measured using a sensION5 conductivity meter (Hach). The air (V_a) and brine (V_b) volume fractions in bulk sea ice were calculated from temperature and salinity of bulk ice following the empirical equations described in Petrich and Eicken[12] (see SI for details).

Data were described using nonparametric statistics, as several variables (sea ice temperature, Hg_T, $MeHg_T$, and DOC) failed the test for normality ($p < 0.05$ for Shapiro−Wilk test). General statistical tests were performed with SigmaPlot v11.0 (Systat Software), while correlation and regression analyses, groupings and curve estimations were performed in SPSS Statistics v20 (IBM).

RESULTS

The profiles of Hg_T and $MeHg_T$ in bulk sea ice, along with temperature, salinity and other ancillary measurements, of MY ice cores from the three study sites are shown in Figure 2. A summary of the data is presented in Table 1. Unless otherwise specified, all the concentrations are reported as per liter of melted bulk sea ice.

Site MY2. The ice temperature and salinity were ∼−1 °C and <5, respectively, throughout most of the core (Figure 2k), suggesting that this ice was in the late melt stage at the time of sampling. The reduced surface salinity and the general linear increase in salinity with depth are characteristic of MY ice, resulting from flushing with snow and ice meltwater produced at the ice surface during the melt season.[30−32] The enriched $\delta^{18}O$ values in the top 30 cm of the core (Figure 2m) further suggest that the meltwater is more likely from the ablation of the bulk ice crystals themselves instead of from snow which would have a more depleted $\delta^{18}O$ signal. Another feature of this core is observed at depths between 210 and 280 cm, whereby $\delta^{18}O$ decreased sharply to −2.5‰ with a corresponding increase in salinity and temperature. This is indicative of a slush ice layer, likely related to seawater intrusion through ice ridging events.[33] The DOC concentrations were low, ranging from 15 to 110 μM, with the highest values in the mid to bottom sections of the core (Figure 2n). The Chl *a* concentrations were very low in the top 200 cm of the core (<0.05 μg L^{-1}) but increased sharply to >4 μg L^{-1} in the bottom 50 cm (Figure 2n). The DOC and Chl *a* profiles are similar to those observed from a MY ice floe in Fram Strait.[32]

Along the 370 cm of the core, elevated Hg_T concentrations were found within the top 40 cm, which is composed of superimposed white ice, with the highest value of 49.2 pM occurring approximately 35 cm from the ice surface (Figure 2h). Within the midsection (40−310 cm) of the core, Hg_T

dx.doi.org/10.1021/es5008033 | Environ. Sci. Technol. 2014, 48, 5575−5582

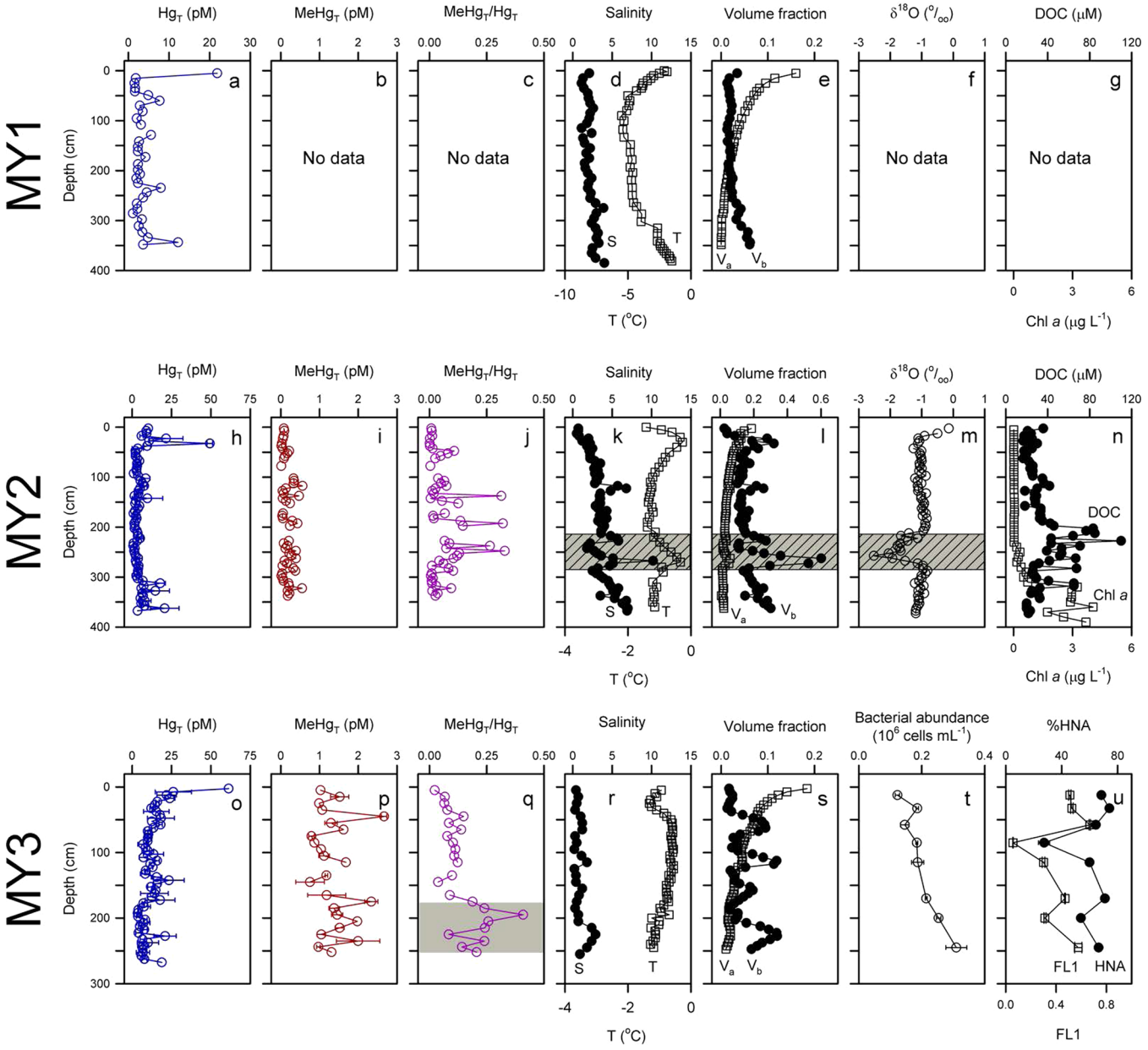

Figure 2. Profiles of total mercury (Hg_T), total methylated mercury ($MeHg_T$), the ratio of $MeHg_T/Hg_T$, bulk salinity (S), temperature (T), and calculated air and brine volume fractions (V_a and V_b, respectively) in multiyear ice at sites MY1 (a–g, based on an earlier study[14]), MY2 (h–n) and MY3 (o–u). Ancillary profiles of $\delta^{18}O$, dissolved organic carbon (DOC), and chlorophyll *a* (Chl *a*) are also shown for site MY2, and those of bacterial abundance, % high nucleic acid content (%HNA), and green fluorescence intensity (FL1) are shown for site MY3. Error bars in panels h, i, o, and p represent the half range of two pseudoreplicate measurements, and those in t and u are standard deviations. The hatched gray area in k, l, and m shows the depths where slush ice was present. The gray area in q shows the depths with high $MeHg_T/Hg_T$ ratios, suggesting the potential occurrence of in situ mercury methylation.

levels dropped to a mean value of 3.19 pM and then increased to a mean of 8.97 pM within the bottom 50 cm. The overall range of the Hg_T concentration (0.65–49.2 pM; median: 3.64 pM) was similar to that reported at MY1 (1.10–21.8 pM, median: 2.79 pM)[14] (Figure 2a).

$MeHg_T$ concentrations were below or near the MDL of 0.1 pM at ~30% of the depths, especially in the top 100 cm of the core (Figure 2i). Higher concentrations up to 0.55 pM were detected in a few sections in the mid to bottom layers of the core. The ratio of $MeHg_T$ to Hg_T ranged from 0 up to 33% at a few depths in the middle section of the core (Figure 2j). The slush ice layer at 210–280 cm had no noticeable effect on Hg_T or $MeHg_T$ concentrations.

Site MY3. Ice temperature (−1.5 to −0.5 °C) and salinity (<3) profiles were fairly homogeneous at MY3, with temperature and salinity being maximum in the middle section and in bottom layer, respectively (Figure 2r). The low salinity values indicate that this ice has experienced a considerable amount of snow meltwater flushing. Arctic summer sea ice melt has been shown to end around mid-August.[12,34] Hence, at the time of sampling (September 9), the MY ice at MY3 was likely experiencing the initial ice growth stage. $\delta^{18}O$, DOC, and Chl *a* were not analyzed at this site. Flow cytometry results showed a

dx.doi.org/10.1021/es5008033 | *Environ. Sci. Technol.* 2014, 48, 5575–5582

gradual increase in total bacterial abundance along the ice core, ranging from 0.2 × 10^6 cells mL^{-1} in the top 25 cm to 0.45 × 10^6 cells mL^{-1} at the deepest layer (Figure 2t), which is similar to the values reported for the bottom 5 cm of FY ice[24] and seawater[35] from the Amundsen Gulf. Bacteria in the top and bottom ice layers showed higher HNA content and FL1 intensity than those in the midsection of the ice (Figure 2u).

The Hg_T concentration ranged from 3.39−60.8 pM at this site (median: 10.9 pM), with the highest concentration (60.8 pM) in the topmost 5 cm layer, decreasing sharply to <25 pM downward (Figure 2o). Excluding the top and bottom layers, Hg_T concentrations were overall 2−3 times higher than at MY1 (Figure 2a) and MY2 (Figure 2h) (Table 1). Similarly, much higher $MeHg_T$ concentrations were measured throughout all the depths at MY3, ranging from 0.75 to 2.64 pM, well above the MDL (Figure 2p, Table 1). The ratio of $MeHg_T$ to Hg_T ranged from 2.3% to 40.9%, with a consistent enrichment in the bottom 100 cm of the ice, peaking at a depth of 195 cm below the ice−air interface (Figure 2q).

DISCUSSION

Processes Driving Hg_T Distribution in MY Ice. The surface enrichment of Hg_T in the MY ice at MY2 and MY3 is in agreement with our earlier study at MY1 collected from a similar region (Figure 2a),[14] as well as with what has been reported in FY ice.[14,15] We have recently shown that Hg_T distribution in FY ice is driven primarily by freeze rejection of seawater Hg in sea ice brine, by snow meltwater flushing, and by the dynamics of particulate matter.[14] The same, however, does not hold true for MY ice. Different from FY ice, the evolution of MY ice through the melt season results in severe desalination and crystal retexturing of the frazil ice layer,[16] and eventually the surface ice morphs into consolidated white ice with little to no brine pockets, yet particulate matter may be retained. As shown in Figure 2e,l,s, the brine volume fraction in the surface layers of MY ice approached zero. Contrary to FY ice where brine concentration of Hg_T was found to correlate with brine salinity,[14] such a relationship does not apply to any of the three MY ice sites (see Figure S1 in SI).

Therefore, the surface peak of Hg_T cannot be accounted for by the freeze rejection of seawater; instead, particulate matter that is entrained in the ice may have played a more important role. Beaufort Sea MY ice is known to entrap fine-grained particulates through scavenging of suspended sediment in the water column by the newly forming frazil ice ("suspension freezing").[36] Particulate matter, from either soil, sediment, snow, or other aerosol sources, tends to accumulate in the surface layer of the ice[31,36] after several seasons of bottom freezing and melting of snow and surface ice.[36] Diatoms and other algae grown in melt ponds also add biogenic particulate matter to surface ice.[36] The surface layer of MY ice has been shown to contain particulate matter concentrations ranging from 0.5 to 900 mg L^{-1} in the Beaufort Gyre,[36] and 0 to 2000 mg L^{-1} along a trans-Arctic Ocean transect from the Chukchi Sea to Barents Sea.[31] We did not collect particulate matter from our cores for Hg analysis. However, using a mean particulate matter concentration in Arctic MY ice of 250 mg L^{-1},[31] the peak values of Hg_T in MY ice observed (~50 pM) can be fully accounted for if the Hg_T content in the particulate matter is ~200 pmol g^{-1}, a value that agrees very well with the Hg_T content of surface sediment in the Arctic Ocean (170−580 pmol g^{-1}).[37]

Elevated Hg_T concentrations were also observed in the bottom ice layer, though not nearly as high as the surface peak. This could be due to the presence of Hg-containing biogenic particles. The profile of Chl *a* as a function of depth at MY2 (Figure 2n) revealed that autotrophic biomass (or relics of this biomass) was found between 240 and 350 cm (at the bottom of the core). Within this section, Chl *a* demonstrated a very strong, positive correlation with Hg_T (r_s = 0.945, p < 0.0005, n = 13), explaining in part the variability in bottom ice Hg_T concentrations. Marine algae take up Hg from their surroundings via absorption, adsorption, and/or through metabolic activity.[38−40] Recent work has reported that the particulate-bound Hg (Hg_p) in the bottom sections of FY ice in the Beaufort Sea ranged from 20 to 110 pmol g^{-1} (dw) during the spring ice algal bloom season (March−May).[38] As the abundance of eukaryotic cells increased over the bloom, concentrations of Hg_p decreased, implying the occurrence of biodilution. Biodilution is not likely to occur to the same extent in MY ice due to much lower algal biomass when compared with the FY ice sampled in that study. The continual drainage of brine and meltwater enriched in Hg_p and subsequent sorption of Hg onto/into the small amount of algal cells or biological fluids could have contributed to the large Hg_T values in the bottom layer ice at MY2.

It should be noted that the three MY ice cores were taken at different locations in different seasons. A Kruskal−Wallis test revealed that there was no statistical difference in Hg_T distribution between MY1 and MY2 (p = 0.49), but Hg_T concentrations at both sites were statistically, significantly lower than those at MY3 (p < 0.001). The similarity in vertical profiles of Hg_T concentrations at MY1 and MY2, both from the eastern Beaufort Sea but in different seasons (MY1 in May 2008; MY2 in August 2011), suggests that the difference between the site in McClure Strait (MY3) and those in the Beaufort Sea (MY1 and MY2) is due to spatial variations.

To understand the higher Hg_T concentrations at MY3, the history of the MY ice within the Beaufort Sea and McClure Strait must be reviewed. Studies of MY ice dynamics from 1968 to 2006 revealed that in most years there is a net export of MY ice from McClure Strait into the Beaufort Sea,[41,42] and that the MY ice of McClure Strait is primarily imported through the Canadian Arctic Archipelago from the northern Queen Elizabeth Islands (QEI) region.[43] When traveling through the Archipelago, floes can become land fast or grounded, which may trap sediment into the bulk sea ice matrix and lead to substantial sediment loadings.[41,44] Seawater profiling at a site near MY3 indeed showed higher Hg_T, as well as $MeHg_T$, than other sites in the Beaufort Sea.[7]

$MeHg_T$ Distribution in MY Ice. To our knowledge, this study represents the first measurements of $MeHg_T$ in MY ice (Figure 2i,p). While $MeHg_T$ concentrations in MY2 are generally low and often near the MDL, much higher $MeHg_T$ concentrations, up to 30 times MDL, are found in MY3 where Hg_T concentrations are also much higher overall. Indeed, at both sites, the ratio of $MeHg_T/Hg_T$ varied in a similar range (0−40%; Figure 2j,q). Of particular interest is the much higher $MeHg_T/Hg_T$ ratios in the mid (Figure 2j) to bottom (Figure 2q) sections of the ice cores. This is most obvious at MY3 where the bottom 180−250 cm of the core consistently had a $MeHg_T/Hg_T$ ratio above 20% (shaded layer in Figure 2q). In the only other study of MeHg in sea ice, albeit in Antarctic landfast FY ice, $MeHg_T$ was also found to peak in the bottom layer of the ice, though at much lower concentrations

dx.doi.org/10.1021/es5008033 | Environ. Sci. Technol. 2014, 48, 5575−5582

(maximum 0.5 pM, $MeHg_T/Hg_T$ = 9.8%).[15] The high $MeHg_T$ concentrations and the distinct depth distribution pattern of $MeHg_T/Hg_T$ in MY ice thus raise an important question on the origin of $MeHg_T$: is it transported from seawater and/or snow, or is it formed in situ within the ice?

Because the distribution pattern of $MeHg_T$ in MY ice does not follow that of Hg_T, it cannot be driven by the same processes that drive the distribution of Hg_T (e.g., particle dynamics as discussed above). Incorporation of seawater $MeHg_T$ into MY ice by freeze rejection is certainly possible but does not appear to be sufficient to explain the high $MeHg_T$ levels observed in MY3 (see also Figure S1 in SI). Our recent measurements of $MeHg_T$ in the Beaufort Sea have revealed that $MeHg_T$ in the water column peaks at the subsurface, ∼150 m below the sea surface, and that $MeHg_T$ concentration in surface seawater is almost completely depleted.[7] Similarly, while $MeHg_T$ has been measured in the Arctic snow cover,[21−23] percolation of snow meltwater cannot explain the presence of a $MeHg_T/Hg_T$ peak only in the mid to bottom layer of the MY ice. Photochemical processes such as Hg(II) photoreduction, Hg(II) photomethylation, and MeHg photodegradation[19,20] could also alter the $MeHg_T/Hg_T$ ratio but are not expected to occur to any significant extent in the mid to bottom layer of the MY ice due to strong attenuation of UV radiation by sea ice.[45]

It is thus plausible that MeHg might be formed in situ in the mid to bottom layer of MY ice. Although there has been no report of known Hg methylators such as sulfate reducing bacteria and iron reducing bacteria in sea ice, anaerobic conditions have been reported in FY sea ice.[17,18] There are also indications that certain aerobic bacteria might also be capable of methylating Hg.[19,22] A recent study has shown that both the richness and diversity of the microbial community in the Arctic MY ice are higher than previously thought.[46] We did not attempt to identify Hg methylating bacteria in this study. Nevertheless, bacterial enumeration was carried out for the MY ice at MY3. As shown in Figure 2t,u, there is a gradual increase in the total number of bacteria toward the bottom section of the ice core. Because total abundance comprises both active and inactive or dead cells, we further investigated bacterial structure at a finer resolution. Although there is no consensus on the ecological and functional significance of HNA populations,[47] the proportion of HNA content cells has been generally considered as the active fraction of the community.[48] The higher FL1 intensity also indicates higher single-cell activity in the bottom section of the ice. Although not statistically correlated throughout the core, the bottom ice section (150−250 cm) where the $MeHg_T/Hg_T$ ratio was the highest (Figure 2q) also had higher bacterial abundance (Figure 2t) with higher %HNA and FL1 (Figure 2u). Also noteworthy is that the sections of the ice core with major changes in $MeHg_T$ concentration (Figure 2p) also corresponded to major changes in the structure of bacterial communities as shown by variations in the level of FL1 and %HNA (Figure 2n). These suggest that in situ microbial Hg methylation in MY ice is highly possible. Further molecular and metagenomics studies are needed to confirm the occurrence of Hg methylation in MY ice and to identify the methylators. If confirmed, the occurrence of in situ Hg methylation in MY ice could have major implications for Hg cycling in the Arctic Ocean.

Flux of Hg_T and $MeHg_T$ into the Arctic Ocean upon Melt of MY Ice. On the basis of the data presented in Figure 2 and Table 1, here we provide the first attempt to estimate the flux of Hg_T and $MeHg_T$ released into the Arctic Ocean system upon melting of MY ice. We recognize that the three MY sites are far from sufficient to extrapolate to the entire Arctic Ocean MY icescape; however, given the extreme logistic challenge (see Acknowledgment) in accessing Arctic MY icepack, such a first-order estimate should still be of value for the understanding of biogeochemical cycles of Hg in the Arctic Ocean. Note that our estimate is for the release of Hg_T and $MeHg_T$ through the complete melt of MY ice; we did not consider the efflux or removal of Hg_T and $MeHg_T$ from the ocean surface during subsequent FY ice formation and growth, nor did we consider the age difference in MY ice.

The volume of MY ice loss over a given melt season was estimated based on the Pan-Arctic Ice Ocean Modeling and Assimilation System (PIOMAS),[49,50] which is a numerical model with inputs for sea ice concentrations, sea surface temperatures, and other observations. The uncertainty of the monthly averaged ice volume is estimated at $\sim 0.75 \times 10^3$ km^3.[49] Monthly mean ice volume data for September, the month during which sea ice extent is at a minimum and the icescape is assumed to be entirely composed of MY ice, are used. The difference in sea ice volume in September from one year to the next represents the net annual loss of MY ice to melt processes. This calculation yielded a mean annual loss in MY ice volume of 280 km^3 yr^{-1}. Taking the mean volume-weighted MY ice Hg_T and $MeHg_T$ concentrations of 7.4 pM and 0.75 pM, respectively, calculated as the mean of the volume-weighted mean bulk sea ice at each of the three sites (Table 1), this amounts to a Hg_T flux of 2.1 kmol yr^{-1} (or 420 kg Hg yr^{-1}) and a $MeHg_T$ flux of 0.21 kmol yr^{-1} (or 42 kg Hg yr^{-1}) into the Arctic Ocean upon MY ice melt.

The magnitude of the Hg_T flux is in agreement with a recent estimate of an influx of ∼0.24 kmol yr^{-1} of Hg_p into the Arctic Ocean with the complete replacement of MY ice with FY ice in the Beaufort Sea,[38] which was based on Hg_T concentrations found within sea ice algae in the bottom 10 cm of thick FY ice. Assuming that all the Hg_T present in the snow over Arctic sea ice makes its way into the ocean, an earlier study estimated Hg_T flux from snowmelt to the Arctic Ocean could be as high as 44 kmol yr^{-1} (or 8800 kg Hg yr^{-1}).[3] While that assumption might be valid for snow over FY ice, much of the snowmelt Hg over the MY ice is entrained in the surface layer of the ice and may not be released into the ocean until the complete melt of the MY ice. Therefore, attenuated by MY ice, the actual annual snowmelt Hg flux to the Arctic Ocean is likely much lower than previously estimated.

Furthermore, in situ methylation of Hg in MY ice, if confirmed, would represent a new substantial source of MeHg that was previously unaccounted for. Through uptake by sea ice algae and water column phytoplankton, sea ice MeHg could act as an effective pathway for MeHg bioaccumulation in the Arctic marine ecosystems. No measurement has been made on MeHg in Arctic FY ice. Assuming that the MeHg concentration in Arctic FY ice is similar to the low values reported for the Antarctic FY ice,[15] a shift from a MY to a FY sea ice regime in the Arctic Ocean would imply a decreasing MeHg production from the sea ice environment.

■ ASSOCIATED CONTENT

Supporting Information

Details of the study area, the analytical methods, the method for estimating air and brine volume fractions and brine concentrations of Hg_T and $MeHg_T$, and one figure as described

dx.doi.org/10.1021/es5008033 | Environ. Sci. Technol. 2014, 48, 5575−5582

in the text. This material is available free of charge via the Internet at http://pubs.acs.org.

AUTHOR INFORMATION

Corresponding Author

*Tel: +1-204-474-6250, fax: +1-204-272-1532, e-mail: feiyue.wang@umanitoba.ca.

Notes

The authors declare no competing financial interest.

ACKNOWLEDGMENTS

This project was supported by funding from the ArcticNet (Network of Centers of Excellence of Canada), the Natural Sciences and Engineering Research Council of Canada, Canada Foundation for Innovation, and the Northern Scientific Training Program of Indian and Northern Affairs Canada. We thank K. Warner, D. Isleifson, L. Candlish, M. Pind, J. S. Côté, M. Simard, C. Lovejoy, and I. Laurion for their assistance in field sampling and laboratory analysis, and the entire crew of the CCGS Amundsen for their assistance with field logistics. The DOC Consensus Reference Materials were generously provided by D. A. Hansell and W. Chen (University of Miami, Miami, FL). We would like to dedicate this paper to the memory of our friends and colleagues Captain Marc Thibault of the Canadian Coast Guard, helicopter pilot Daniel Dubé of Transport Canada, and Dr. Klaus Hochheim of the University of Manitoba, who died tragically in the McClure Strait following the crash of the CCGS Amundsen's helicopter on September 9, 2013, shortly after helping us collect the ice core at MY3.

REFERENCES

(1) AMAP. *AMAP Assessment 2011: Mercury in the Arctic*; Arctic Monitoring and Assessment Program, Oslo, Norway, 2011.

(2) AMAP. *AMAP Assessment 2009: Human Health in the Arctic*; Arctic Monitoring and Assessment Program, Oslo, Norway, 2009.

(3) Outridge, P. M.; Macdonald, R. W.; Wang, F.; Stern, G. A.; Dastoor, A. P. A mass balance inventory of mercury in the Arctic Ocean. *Environ. Chem.* **2008**, *5*, 89−111.

(4) Wang, F.; Macdonald, R. W.; Stern, G. A.; Outridge, P. M. When noise becomes the signal: Chemical contamination of aquatic ecosystems under a changing climate. *Mar. Pollut. Bull.* **2010**, *60*, 1633−1635.

(5) Macdonald, R. W.; Harner, T.; Fyfe, J. Recent climate change in the Arctic and its impact on contaminant pathways and interpretation of temporal trend data. *Sci. Total Environ.* **2005**, *342*, 5−86.

(6) Stern, G. A.; Macdonald, R. W.; Outridge, P. M.; Wilson, S.; Chetelat, J.; Cole, A.; Hintelmann, H.; Loseto, L. L.; Steffen, A.; Wang, F.; Zdanowicz, C. How does climate change influence arctic mercury? *Sci. Total Environ.* **2012**, *414*, 22−42.

(7) Wang, F.; Macdonald, R.; Armstrong, D.; Stern, G. Total and methylated mercury in the Beaufort Sea: The role of local and recent organic remineralization. *Environ. Sci. Technol.* **2012**, *46*, 11821−11828.

(8) Comiso, J. C. Large decadal decline of the Arctic multiyear ice cover. *J. Clim.* **2012**, *25*, 1176−1193.

(9) Maslanik, J.; Fowler, C.; Stroeve, J.; Drobot, S.; Zwally, J.; Yi, D.; Emery, W. A younger, thinner Arctic ice cover: Increased potential for rapid, extensive sea-ice loss. *Geophys. Res. Lett.* **2007**, *34*, L24501, doi: 10.1029/2007GL032043.

(10) Maslanik, J.; Stroeve, J.; Fowler, C.; Emery, W. Distribution and trends in Arctic sea ice age through spring 2011. *Geophys. Res. Lett.* **2011**, *38*, L13502, doi: 10.1029/2011GL047735.

(11) Nghiem, S. V.; Rigor, I. G.; Perovich, D. K.; Clemente-Colon, P.; Weatherly, J. W.; Neumann, G. Rapid reduction of Arctic perennial sea ice. *Geophys. Res. Lett.* **2007**, *34*, L19504, doi: 10.1029/2007GL031138.

(12) Petrich, C.; Eicken, H. Growth, structure and properties of sea ice. In *Sea Ice*, 2nd ed.; Thomas, D. N.; Dieckmann, G. S., Eds.; Wiley-Blackwell: Chichester, UK, 2010; pp 23−77.

(13) Thomas, D. N.; Papadimitriou, S.; Michel, C. Biogeochemistry of Sea Ice. In *Sea Ice*, 2nd ed.; Thomas, D. N.; Dieckmann, G. S., Eds.; Wiley-Blackwell: Chichester, UK, 2010; pp 425−467.

(14) Chaulk, A.; Stern, G. A.; Armstrong, D.; Barber, D.; Wang, F. Mercury distribution and transport across the ocean − sea-ice − atmosphere interface in the Arctic Ocean. *Environ. Sci. Technol.* **2011**, *45*, 1866−1872.

(15) Cossa, D.; Heimbuerger, L.-E.; Lannuzel, D.; Rintoul, S. R.; Butler, E. C. V.; Bowie, A. R.; Averty, B.; Watson, R. J.; Remenyi, T. Mercury in the Southern Ocean. *Geochim. Cosmochim. Acta* **2011**, *75*, 4037−4052.

(16) Tucker, W. B.; Perovich, D.; Gow, A. J.; Weeks, W. F.; Drinkwater, M. R. Physical properties of sea ice relevant to remote sensing. In *Microwave Remote Sensing of Sea Ice*; Carsey, F. D., Ed.; American Geophysical Union: Washington, DC, 1992; pp 9−26.

(17) Rysgaard, S.; Glud, R. N. Anaerobic N_2 production in Arctic sea ice. *Limnol. Oceanogr.* **2004**, *49*, 86−94.

(18) Rysgaard, S.; Glud, R. N.; Sejr, M. K.; Blicher, M. E.; Stahl, H. J. Denitrification activity and oxygen dynamics in Arctic sea ice. *Polar Biol.* **2008**, *31*, 527−537.

(19) Barkay, T.; Kroer, N.; Poulain, A. J., Some like it cold: Microbial transformations of mercury in polar regions. *Polar Res.* **2011**, *30*.

(20) Lehnherr, I.; St Louis, V. L.; Hintelmann, H.; Kirk, J. L. Methylation of inorganic mercury in polar marine waters. *Nature Geosci.* **2011**, *4*, 298−302.

(21) St Louis, V. L.; Hintelmann, H.; Graydon, J. A.; Kirk, J. L.; Barker, J.; Dimock, B.; Sharp, M. J.; Lehnherr, I. Methylated mercury species in Canadian high arctic marine surface waters and snowpacks. *Environ. Sci. Technol.* **2007**, *41*, 6433−6441.

(22) Larose, C.; Dommergue, A.; De Angelis, M.; Cossa, D.; Averty, B.; Marusczak, N.; Soumis, N.; Schneider, D.; Ferrari, C. Springtime changes in snow chemistry lead to new insights into mercury methylation in the Arctic. *Geochim. Cosmochim. Acta* **2010**, *74*, 6263−6275.

(23) Lahoutifard, N.; Sparling, M.; Lean, D. Total and methyl mercury patterns in Arctic snow during springtime at Resolute, Nunavut, Canada. *Atmos. Environ.* **2005**, *39*, 7597−7606.

(24) Nguyen, D.; Maranger, R. Respiration and bacterial carbon dynamics in Arctic sea ice. *Polar Biol.* **2011**, *34*, 1843−1855.

(25) Fitzgerald, W. F. Clean hands, dirty hands: Clair Patterson and the aquatic biogeochemistry of mercury. In *Clean Hands, Clair Patterson's Crusade Against Environmental Lead Contamination*; Davidson, C. I., Ed.; Nova Science: Commack, NY, 1999; pp 119−137.

(26) Burdige, D. J.; Homstead, J. Fluxes of dissolved organic carbon from Chesapeake Bay sediments. *Geochim. Cosmochim. Acta* **1994**, *58*, 3407−3424.

(27) U.S. EPA. *Method 1631, Revision E: Mercury in water by oxidation, purge and trap, and cold vapor atomic fluorescence spectrometry*; U.S. Environmental Protection Agency, Washington, DC, 2002.

(28) U.S. EPA. *Method 1630. Methyl Mercury in Water by Distillation, Aqueous Ethylation, Purge and Trap, and CVAFS*; U.S. Environmental Protection Agency, Washington, DC, 2001.

(29) Bowman, K. L.; Hammerschmidt, C. R. Extraction of monomethylmercury from seawater for low-femtomolar determination. *Limnol. Oceanogr. Methods* **2011**, *9*, 121−128.

(30) Eicken, H.; Lensu, M.; Leppäranta, M.; Tucker, W. B.; Gow, A. J.; Salmela, O. Thickness, structure, and properties of level summer multiyear ice in the Eurasian sector of the Arctic Ocean. *J. Geophys. Res.* **1995**, *100* (C11), 22697−22710.

(31) Tucker, W. B.; Gow, A. J.; Meese, D. A.; Bosworth, H. W.; Reimnitz, E. Physical characteristics of summer sea ice across the Arctic Ocean. *J. Geophys. Res. Oceans* **1999**, *104* (C1), 1489−1504.

(32) Thomas, D. N.; Lara, R. J.; Eicken, H.; Kattner, G.; Skoog, A. Dissolved organic matter in Arctic multi-year sea ice during winter: major components and relationship to ice characteristics. *Polar Biol.* **1995**, *15*, 477−483.
(33) Toyota, T.; Takatsuji, S.; Tateyama, K.; Naoki, K.; Ohshima, K. I. Properties of sea ice and overlying snow in the southern Sea of Okhotsk. *J. Oceanogr.* **2007**, *63*, 393−411.
(34) Eicken, H.; Krouse, H.; Kadko, D.; Perovich, D. Tracer studies of pathways and rates of meltwater transport through Arctic summer sea ice. *J. Geophys. Res.* **2002**, *107* (C10), 8046, doi: 10.1029/2000JC000583.
(35) Alonso-Sáez, L.; Sanchez, O.; Gasol, J. M.; Balague, V.; Pedrós-Alió, C. Winter-to-summer changes in the composition and single-cell activity of near-surface Arctic prokaryotes. *Environ. Microbiol.* **2008**, *10*, 2444−2454.
(36) Reimnitz, E.; Barnes, P. W.; Weber, W. S. Particulate matter in pack ice of the Beaufort Gyre. *J. Glaciol.* **1993**, *39*, 186−198.
(37) Gobeil, C.; Macdonald, R. W.; Smith, J. N. Mercury profiles in sediments of the Arctic Ocean basins. *Environ. Sci. Technol.* **1999**, *33*, 4194−4198.
(38) Burt, A.; Wang, F.; Pućko, M.; Mundy, C.-J.; Gosselin, M.; Philippe, B.; Poulin, M.; Tremblay, J. E.;Stern, G. A. Mercury uptake within an ice algal community during the spring bloom in first-year Arctic sea ice. *J. Geophys. Res. Oceans* **2013**, *118*, doi: 10.1002/jgrc.20380.
(39) Mason, R. P.; Reinfelder, J. R.; Morel, F. M. M. Uptake, toxicity, and trophic transfer of mercury in a coastal diatom. *Environ. Sci. Technol.* **1996**, *30*, 1835−1845.
(40) Herrero, R.; Lodeiro, P.; Rey-Castro, C.; Vilariño, T.; Sastre de Vicente, M. E. Removal of inorganic mercury from aqueous solutions by biomass of the marine macroalga *Cystoseira baccata*. *Water Res.* **2005**, *39*, 3199−3210.
(41) Kwok, R. Exchange of sea ice between the Arctic Ocean and the Canadian Arctic Archipelago. *Geophys. Res. Lett.* **2006**, *33*, L16501, doi: 10.1029/2006GL027094.
(42) Howell, S. E.; Tivy, A.; Yackel, J. J.; McCourt, S. Multi-year sea-ice conditions in the western Canadian arctic archipelago region of the northwest passage: 1968−2006. *Atmos. Ocean* **2008**, *46*, 229−242.
(43) Howell, S. E.; Duguay, C. R.; Markus, T. Sea ice conditions and melt season duration variability within the Canadian Arctic Archipelago: 1979−2008. *Geophys. Res. Lett.* **2009**, *36*, L10502, doi: 10.1029/2009GL037681.
(44) Pfirman, S.; Eicken, H.; Bauch, D.; Weeks, W. F. The potential transport of pollutants by Arctic sea ice. *Sci. Total Environ.* **1995**, *159*, 129−146.
(45) Perovich, D. K. *The Optical Properties of Sea Ice. CRREL Monograph, 96-1*; Cold Regions Research and Engineering Laboratory, Hanover, NH, 1996; p 25.
(46) Bowman, J. S.; Rasmussen, S.; Blom, N.; Deming, J. W.; Rysgaard, S.; Sicheritz-Ponten, T. Microbial community structure of Arctic multiyear sea ice and surface seawater by 454 sequencing of the 16S RNA gene. *ISME J.* **2012**, *6*, 11−20.
(47) Bouvier, T.; del Giorgio, P. A.; Gasol, J. M. A comparative study of the cytometric characteristics of high and low-nucleic-acid bacterioplankton cells from different aquatic ecosystems. *Environ. Microbiol.* **2007**, *9*, 2050−2066.
(48) Lebaron, P.; Servais, P.; Agogué, H.; Courties, C.; Joux, F. Does the high nucleic acid content of individual bacterial cells allow us to discriminate between active cells and inactive cells in aquatic systems? *Appl. Environ. Microbiol.* **2001**, *67*, 1775−1782.
(49) Schweiger, A.; Lindsay, R.; Zhang, J.; Steele, M.; Stern, H.; Kwok, R. Uncertainty in modeled Arctic sea ice volume. *J. Geophys. Res.* **2011**, *116*, C00D06, doi: 10.1029/2011JC007084.
(50) Zhang, J.; Rothrock, D. A. Modeling global sea ice with a thickness and enthalpy distribution model in generalized curvilinear coordinates. *Monthly Weather Rev.* **2003**, *131*, 845−861.